Integrated Design of Agile Missile Guidance and Autopilot Systems

By

P. K. Menon[*] and E. J. Ohlmeyer[++]

Abstract

Recent threat assessments by the US Navy have indicated the need for improving the accuracy of defensive missiles. This objective can only be achieved by enhancing the performance of the missile subsystems and by finding methods to exploit the synergism existing between subsystems. As a first step towards the development of integrated design methodologies, this paper develops a technique for integrated design of missile guidance and autopilot systems. Traditional approach for the design of missile guidance and autopilot systems has been to design these subsystems separately and then to integrate them together before verifying their performance. Such an approach does not exploit any beneficial relationships between these and other subsystems.

The application of the feedback linearization technique for integrated guidance-autopilot system design is discussed in this paper. Numerical results using a six degree-of-freedom missile simulation are given. Integrated guidance-autopilot systems are expected to result in significant improvements in missile performance, leading to lower weight and enhanced lethality. Both of these factors will lead to a more effective, lower-cost weapon system. Integrated system design methods developed under the present research effort also have extensive applications in high performance aircraft autopilot and guidance systems.

1. Introduction

The evolving nature of the threats to the Naval assets have been discussed in the recent literature (Ohlmeyer, 1996; Bibel *et al*., 1994; Chadwick, 1994; Zarchan, 1995). These research efforts have identified very small miss distance as a major requirement for the next generation missiles used in ship defense against tactical ballistic missiles and sea skimming missiles. Two key technologies that have the potential to help achieve this capability are the development of advanced sensors and methods for achieving tighter integration between the

---

[*] Research Scientist, *Optimal Synthesis Inc.*, 450 San Antonio Road, Suite 200, Palo Alto, CA 94306-4646, U. S. A; e_mail: menon@optisyn.com

[++] Research Scientist, Naval Surface Warfare Center, Code G23, Dahlgren, VA 22448, U. S. A; e_mail: eohlmey@nswc.navy.mil.

This research was supported under U. S. Navy Contract No. N00178-97-C-1028.

Paper Presented at the *1999 Mediterranean Control Conference,* June 28-30, Haifa, Israel.

missile guidance, autopilot and fuze-warhead subsystems. This paper presents a preliminary research effort on the integrated design of missile guidance and autopilot system.

Past trend in the missile industry has been to design each subsystem using separate engineering teams and then to integrate them. Modifications are subsequently made to each subsystem in order to achieve the desired weapon system performance. Such an approach can result in excessive design iterations, and may not always exploit any synergism existing between interacting subsystems. This has led to a search for integrated design methods that can help establish design tradeoffs between subsystem specifications early-on in the design iterations. Recent research (Ohlmeyer, 1996) on quantifying the impact of each missile subsystem parameters on the miss distance can serve as the first step towards integrated design of missile guidance and autopilot systems.

Integrated design of the flight vehicle systems is an emerging trend within the aerospace industry. Currently, there are major research initiatives within the aerospace industry, DoD and NASA to attempt inter-disciplinary optimization of the whole vehicle design, while preserving the innovative freedom of individual subsystem designers. Integrated design of guidance, autopilot, and fuze/warhead systems represents a parallel trend in the missile technology.

The block diagram of a missile guidance and autopilot loop is given in Figure 1. The target states relative to the missile estimated by the seeker and a state estimator form the inputs to the guidance system. Typical inputs include target position and velocity vectors relative to the missile. In response to these inputs, and those obtained from the onboard sensors, the guidance system generates acceleration commands for the autopilot. The autopilot uses the guidance commands and sensor outputs to generate commands for the actuator blending logic, which optimally selects a mix of actuators to be used at the given flight conditions. The fuse/warhead subsystem uses the relative location of the target with respect to the missile as the input and responds in such a way as to maximize the warhead effectiveness.

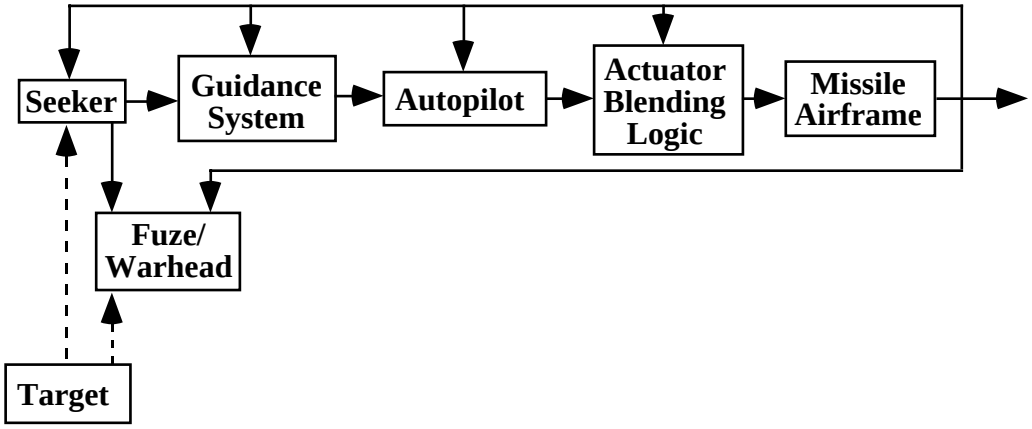

Fig. 1. Block Diagram of an Advanced Missile Guidance, Autopilot, and Fuze/Warhead Systems

Each of these subsystems have interactions that can be used to optimize the performance of the missile system. For instance, missiles with higher accuracy guidance and autopilot systems can employ smaller warheads. Guidance laws that have anticipatory capabilities can reduce the autopilot time response requirements. High bandwidth autopilot can make the guidance system more effective. High quality actuator blending logic can similarly lead to more accurate fuel conservative maneuvers that can enhance the autopilot performance. Similarly, the seeker field of view and speed of response depend on the target agility, and the response of missile guidance and autopilot system.

Traditional approach for designing the missile autopilot and guidance systems has been to neglect these interactions and to treat individual missile subsystems separately. Designs are generated for each subsystem and these subsystems are then assembled together. If the overall system performance is unsatisfactory, individual subsystems are re-designed to improve the system performance. While this design approach has worked well in the past, it often leads to the conservative design of the on-board systems, leading to a heavier, more expensive weapon system.

"Hit-to-kill" capabilities required in the next generation missile system will require a more quantitative design approach in order to exploit synergism between various missile subsystems and thereby guaranteeing the weapon system performance. Integrated system design methods available in the literature (Garg, 1993; Menon *et al*., 1995) can be tailored for designing the missile subsystems.

This paper presents the application of an emerging nonlinear system design method for the integrated design of missile guidance and autopilot systems. Integration of actuator blending logics (Menon *et al*., 1998) and other subsystems will be considered during future

research efforts. The present research employs a six degree-of-freedom nonlinear missile model, and a spiraling point-mass target model. These models are discussed in Section 2. Section 2 also lists the general performance requirements of the integrated guidance-autopilot system design.

Integrated guidance-autopilot system design using the State Dependent Riccati Equation (SDRE) technique (Cloutier *et al*., 1996; Mracek *et al*., 1997; Cloutier, 1997) will be discussed in detail in this paper. The SDRE design technique is based on the State Dependent Coefficient (SDC) form of the missile equations of motion, and provides a stabilizing control law that is optimal with respect to an infinite-time performance index. The SDRE implementation requires the on-line solution of a matrix Riccati equation. Since the SDRE guidance-autopilot law is based on an infinite-time formulation, a command generator is desirable to provide fast response without encountering actuator saturation. The command generator can also be used to meet a terminal aspect angle requirement. Section 3 presents the details of the integrated SDRE guidance-control system design, command generation and performance evaluation. Conclusions from the present research are given in Section 4.

2. Missile Model

A nonlinear six degrees-of-freedom missile model is used for the present research. This model is derived from a high fidelity simulation developed under a previous research effort (Menon *et al*., 1996), and will be further discussed in Section 2.1. The guidance- autopilot system development will include a point-mass target model performing weaving maneuvers. The equations of motion for the target will be given in Section 2.2. Section 2.3 will discuss the performance requirements of the integrated guidance/control law.

2.1. Six Degrees of Freedom Missile Model

A body coordinate system and an inertial coordinate system are used to derive the equations of motion. These coordinate systems are illustrated in Figure 2. The origin of the body axis system is assumed to be at the missile center of gravity. The X_B axis of the body axis system points in the direction of the missile nose, the Y_B axis points in the starboard direction, and the Z_B axis completes the right-handed triad. The missile position and attitude are defined with respect to an earth-fixed inertial frame. The origin of the earth-fixed coordinate system is located at the missile launch point, with the X axis pointing towards the

initial location of the target, and the Z axis pointing along the local gravity vector. The Y axis direction completes the right-handed coordinate system.

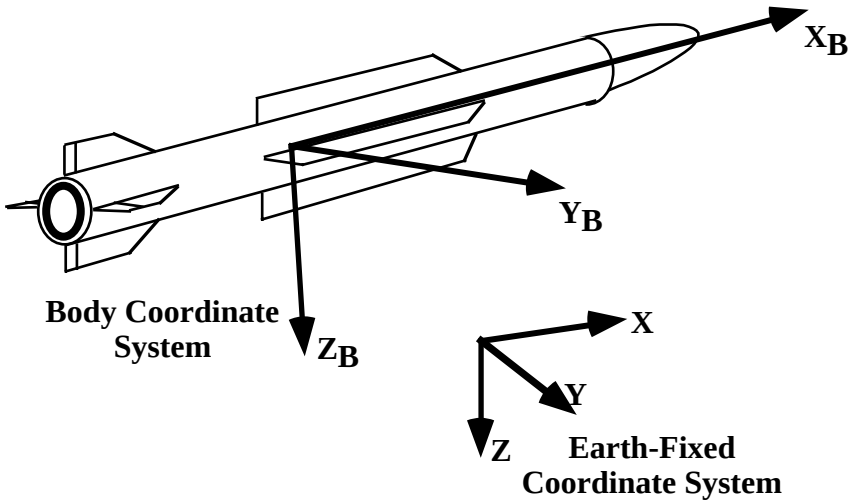

Fig. 2. Missile Coordinate Systems

The translational and rotational dynamics of the missile are described by the following six nonlinear differential equations:

$$\dot{U} = -\frac{\bar{q}s}{m}\begin{bmatrix} a_{0_{C_A}} + a_{1_{C_A}}|\alpha| + a_{2_{C_A}}|\beta| + a_{3_{C_A}}|\alpha\beta| + a_{4_{C_A}}|\delta_Q| + \\ a_{5_{C_A}}|\delta_R| + a_{6_{C_A}}|\delta_P| + a_{7_{C_A}}\delta_Q^2 + a_{8_{C_A}}\delta_R^2 + a_{9_{C_A}}|\delta_Q\delta_R| \end{bmatrix} - WQ + VR + \frac{F_{xg}}{m}$$

$$\dot{V} = \frac{\bar{q}s}{m}\begin{bmatrix} a_{1_{C_Y}}\alpha + a_{2_{C_Y}}\beta + a_{3_{C_Y}}\alpha^3 + a_{4_{C_Y}}\beta^3 + a_{5_{C_Y}}\delta_Q + \\ a_{6_{C_Y}}\delta_R + a_{7_{C_Y}}\delta_P \end{bmatrix} - UR + WP + \frac{F_{yg}}{m}$$

$$\dot{W} = -\frac{\bar{q}s}{m}\begin{bmatrix} a_{1_{C_N}}\alpha + a_{2_{C_N}}\beta + a_{3_{C_N}}\alpha^3 + a_{4_{C_N}}\beta^3 + a_{5_{C_N}}\delta_Q + \\ a_{6_{C_N}}\delta_R + a_{7_{C_N}}\delta_P \end{bmatrix} - VP + UQ + \frac{F_{zg}}{m}$$

$$\dot{P} = \frac{1}{I_x}\bar{q}sl\left[a_{1_{C_l}}\alpha + a_{2_{C_l}}\beta + a_{3_{C_l}}\alpha^3 + a_{4_{C_l}}\beta^3 + a_{5_{C_l}}\delta_Q + a_{6_{C_l}}\delta_R + a_{7_{C_l}}\delta_P\right]$$

$$\dot{Q} = \frac{1}{I_y}\bar{q}sl\left[a_{1_{C_m}}\alpha + a_{2_{C_m}}\beta + a_{3_{C_m}}\alpha^3 + a_{4_{C_m}}\beta^3 + a_{5_{C_m}}\delta_Q + a_{6_{C_m}}\delta_R + a_{7_{C_m}}\delta_P\right] - \frac{(I_x - I_z)}{I_y}PR$$

$$\dot{R} = \frac{1}{I_z}\bar{q}sl\left[a_{1_{C_n}}\alpha + a_{2_{C_n}}\beta + a_{3_{C_n}}\alpha^3 + a_{4_{C_n}}\beta^3 + a_{5_{C_n}}\delta_Q + a_{6_{C_n}}\delta_R + a_{7_{C_n}}\delta_P\right] - \frac{(I_y - I_x)}{I_z}PQ$$

In these equations, U, V, W are the velocity components measured in the missile body axis system; P, Q, R are the components of the body rotational rate; F_{XG}, F_{YG}, F_{ZG} are the gravitational forces acting along the body axes; and I_X, I_Y, I_Z are the vehicle moments of inertia. For Phase I research, it is assumed that the missile body axes coincide with its

principal axes. The aerodynamic force and moment coefficients are described in a polynomial form with respect to angle of attack α, angle of sideslip β, pitch fin deflection δ_Q, yaw fin deflection δ_R, and the roll fin deflection δ_P. The coefficients of the polynomials describing the aerodynamic coefficients were derived by carrying out least squares fits on the aerodynamic data from (Menon and Iragavarapu, 1996). The variable s is the reference area and l is the reference length.

The missile speed V_T , Mach number M, dynamic pressure $\bar{q}$, angle of attack α, and the angle of sideslip β are defined as:

$$V_T = \sqrt{U^2 + V^2 + W^2}\ ,\ M = V_T / a\ ,\ \bar{q} = \frac{1}{2}\rho V_T^2\ ,\ \alpha = \tan^{-1}\left(\frac{W}{U}\right),\ \beta = \tan^{-1}\left(\frac{V}{U}\right)$$

Due to the preliminary nature of the present research, the aerodynamic coefficients are assumed to be independent of the Mach number.

The missile position with respect to the earth-fixed inertial coordinate system can be described by using a coordinate transformation matrix T_{IB} between the body frame and the inertial frame as:

$$\begin{bmatrix} \dot{X} \\ \dot{Y} \\ \dot{Z} \end{bmatrix} = T_{IB} \begin{bmatrix} U \\ V \\ W \end{bmatrix}$$

The coordinate transformation matrix with respect to the Euler angles ψ, θ, ϕ is:

$$T_{IB} = \begin{bmatrix} \cos\theta\cos\psi & \sin\phi\sin\theta\cos\psi - \cos\phi\sin\psi & \cos\phi\sin\theta\cos\psi + \sin\phi\sin\psi \\ \cos\theta\sin\psi & \sin\phi\sin\theta\sin\psi + \cos\phi\cos\psi & \cos\phi\sin\theta\sin\psi - \sin\phi\cos\psi \\ -\sin\theta & \sin\phi\cos\theta & \cos\phi\cos\theta \end{bmatrix}$$

Yaw (ψ), pitch (θ), roll (ϕ) Euler angle sequence is used to derive this transformation matrix. The Euler angle rates with respect to the body rotational rates are given by the expressions:

$$\dot{\theta} = Q\cos\phi - R\sin\phi$$

$$\dot{\phi} = P + Q\sin\phi\tan\theta + R\cos\phi\tan\theta$$

$$\dot{\psi} = (Q\sin\phi + R\cos\phi)\sec\theta$$

Since the missile seeker defines the target position relative to the missile body coordinate system, it is desirable to describe the relative position of the missile with respect to the target in a coordinate system parallel to the instantaneous missile body axis system. For instance, if the target velocity is assumed to be negligible when compared with the

missile velocity, and if the origin of the coordinate system is assumed to be located at the target, the kinematic equations for describing the missile position relative to the target are:

$$\dot{X}_b = U + Y_b R - Z_b Q$$

$$\dot{Y}_b = V - X_b R + Z_b P$$

$$\dot{Z}_b = W + X_b Q - Y_b P$$

The main advantage of describing the target relative missile position in the rotating coordinate system is that it circumvents the need for computing the Euler angles required in the transformation matrix during guidance law computations. In all that follows, the target velocity vector will be assumed to be negligible when compared with the missile velocity vector.

Note that the missile/target position coordinates in this rotating frame can be related to their position vector in the inertial frame using the T_{IB} transformation matrix as:

$$\begin{bmatrix} X \\ Y \\ Z \end{bmatrix} = T_{IB} \begin{bmatrix} X_b \\ Y_b \\ Z_b \end{bmatrix}$$

Second-order fin actuator dynamics from Menon and Iragavarapu (1996) is incorporated in the missile model. However, due to their fast speed of response, these models are not used for integrated control law development or in routine simulations. The reaction jet actuators are not included in the present research. During future work, the actuator blending logics developed in a previous research study (Menon *et al.*, 1997) will be used to integrate the reaction jet actuators in the integrated guidance/control loop.

Although the measurements available on board the missile are limited, the present research will assume that all the measurements required for the implementation of the integrated guidance/control law are available.

2.2. Target Model

Two types of target models are considered in the present research. These are maneuvering and nonmaneuvering targets. The maneuvering targets are assumed to execute weaving maneuvers, and the nonmaneuvering targets are assumed to fly along straight line flight paths.

The maneuvering target model is formulated based on the work of Chadwick (1994) and Zarchan (1995) where it was indicated that tactical ballistic missiles (TBM) exhibit severe

spiraling maneuvers as they reenter earth's atmosphere. The spiral maneuver magnitude is in 1 to 10 g range, with an altitude range of 60 kft to 100 kft. The spiraling frequency range is between 0.5 and 1.0 Hz.

In the present research, the target motions are described in an earth-fixed inertial frame with the Z-axis pointing along the local gravity vector, X-axis pointing towards east, and the Y-axis completing the right-handed triad. The equations of motion of the target are given by:

$$\ddot{X}_T = -A\omega^2 \sin \omega t, \ddot{Y}_T = -A\omega^2 \cos \omega t, \ddot{Z}_T = -g$$

Here, A is the amplitude of the spiral motion in feet, ω is the frequency of the spiral in radians/second, t is the elapsed time in seconds, and g is the acceleration due to gravity. Both the amplitude and frequency of the spiral are assumed to be constant in the present research.

2.3. Integrated Guidance/Control Law Performance Requirements

In traditional flight control systems, the guidance law uses the relative missile/target states to generate acceleration commands. The acceleration commands are generated with the assumption that the missile rotational dynamics is fast enough to be considered negligible. If perfectly followed, these acceleration commands will result in target interception. The autopilot tracks the acceleration commands by changing the missile attitude to generate angle of attack and angle of sideslip using fin deflections and/or moments generated using the reaction jet thrust.

These two functions are combined in integrated guidance/control laws. Integrated guidance/control laws use the target states relative to the missile to directly generate fin deflections that will result in target interception. In addition to achieving target interception, the integrated guidance/control law has the responsibility for ensuring the internal stability of the missile dynamics. Some of the general performance guidelines used during the present research for integrated guidance/control system design are that:

1. It must intercept maneuvering targets with very small miss distances.
2. It must maintain the roll rate near zero throughout the engagement.
3. It must be capable of intercepting the target with a desired terminal aspect angle. The aspect angle may be defined in various ways. For purposes of this research, it is defined as the angle between the missile velocity vector and the target velocity vector, as illustrated in Figure 3.

4. It must stabilize all the states of the missile.

5. It must achieve its objectives while satisfying the position and rate limits on the fin/reaction jet actuators.

6. It must be capable of adapting to small, but rapid changes in target position as may occur during the last few seconds of interception.

Figure 3 illustrates one definition of the terminal aspect angle. This is the angle that the missile velocity vector makes with respect to the target velocity vector at intercept. It is obvious that a good estimate of the target velocity vector with respect to the missile is essential for reliably implementing the terminal aspect angle constraint. Although it is not necessary, for the sake of simplicity, the integrated guidance/control law development will meet the aspect angle constraint separately in the pitch and yaw planes.

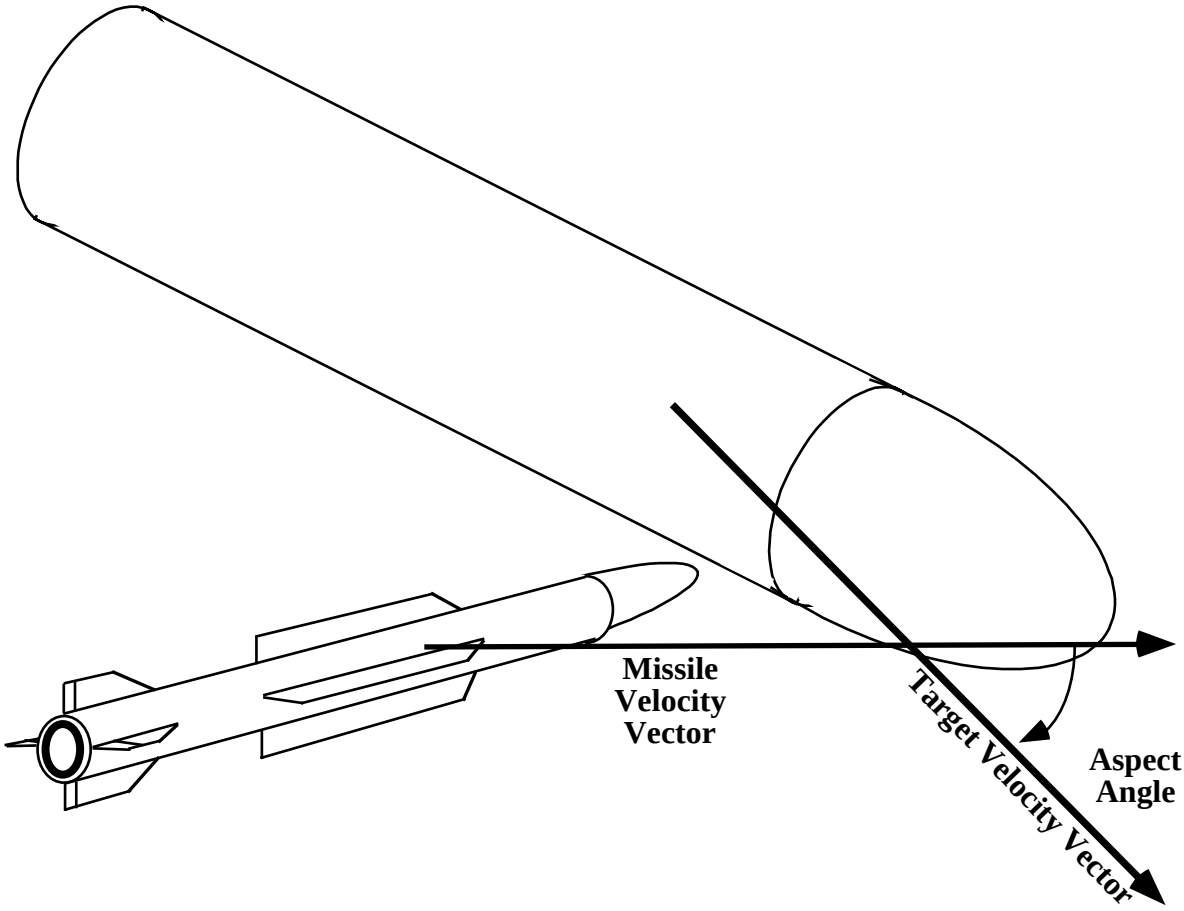

Fig. 3. Aspect Angle at Target Interception

The terminal aspect angle constraint can be satisfied in several different ways. Firstly, the guidance law can be explicitly formulated to meet the terminal aspect angle constraint. While this is the most direct approach, the resulting analytical formulation may be intractable. The approach followed in the present research is based on ensuring that the

relative missile/target lateral velocity component at interception will be a fixed fraction of the relative missile/target longitudinal velocity component. This way, the terminal aspect angle constraint is converted into a constraint on the relative missile/target lateral velocity component at the final time.

Missile/target models discussed in this section form the basis for the development of integrated guidance/control laws in the following section.

3. Integrated Design Using the State Dependent Riccati Equation Method

State Dependent Riccati Equation (SDRE) method (Cloutier *et al*., 1996; Mracek *et al*., 1997; Cloutier, 1997) is a recently emerged nonlinear control system design methodology for direct synthesis of nonlinear feedback controllers. Using a special form of the equations of motion, this approach permits the designer to employ linear optimal control methods such as the LQR methodology and the H• design technique for the synthesis of nonlinear control systems. The application of the SDRE technique for the development of integrated guidance and control system will be discussed in this section. A brief introduction to the SDRE technique will be presented in Section 3.1.

The SDRE design technique requires the dynamic model of the system to be placed in the State Dependent Coefficient (SDC) form. The SDC form has the structure:

$$\dot{x} = A(x)x + B(x)u$$

In its most general form, the SDRE technique allows the inclusion of a disturbance term (Cloutier, *et al*., 1996). In that case, the method is amenable for control law synthesis using the H• technique. However, since the present research does not anticipate using the H• technique for design, this term will be dropped from consideration.

Note that the SDC form has the same structure as a linear dynamic system, but with the system matrix A and the control influence matrix B being functions of the state variables. Cloutier *et al*. (1996) have shown that the SDC form can be derived for most nonlinear dynamic systems using simple algebraic manipulations. That work has also demonstrated that a multivariable system can be parameterized in this manner in an infinite number of ways. Some of these forms may be superior to others in terms of their dynamic behavior near desired points of equilibria.

The SDRE technique uses the equations of motion in the SDC form together with a state dependent quadratic performance index to derive the nonlinear control law. A state dependent algebraic Riccati equation is first formulated using the SDC model and state

dependent weights in the performance index. The solution to the state dependent Riccati equation then yields a state dependent gain matrix that stabilizes the nonlinear system. In the case where all the system states are not available from measurements, the procedure can be modified to synthesize state dependent estimators. If sufficient computational resources are available, the SDRE approach can be extended to include design techniques such as H• and μ-synthesis. The application of the SDRE design technique for integrated guidance/control system design will be discussed in Section 3.3, together with simulation results.

Since the SDRE approach solves the infinite time-horizon control problem, the resulting controller will have purely reactive characteristics. As a result, the controller will attempt to immediately correct any errors in the control loop. This property can lead to actuator saturation when the missile is far away from the target. Moreover, the infinite time-horizon nature of the SDRE solution makes it difficult to meet terminal boundary conditions. One such boundary condition of interest is the terminal aspect angle. These difficulties can be circumvented by using a command generator. The command generator can then be considered as an additional design degree of freedom. Note that the command generator can be considered to be the input compensator in a two degree-of-freedom design procedure (Wolovich, 1994), currently gaining acceptance in the robust-linear control community. Two degree-of-freedom design technique allows the designer to independently shape the tracking performance and the closed-loop behavior of automatic control systems. The synthesis of a simple command generator that accomplishes target interception while achieving a desired terminal aspect angle is discussed in Section 3.3. Evaluation of the integrated guidance/control system for three interception scenarios are given in Section 3.4.

3.1. A Summary of the SDRE Design Approach

The SDRE approach was first discussed by Cloutier *et al*. (1996). This approach assumes that the dynamic model of the system under consideration can be placed in the SDC form discussed at the beginning of Section 3. The second ingredient of the SDRE design technique is the definition of a quadratic performance index in state dependent form:

$$J = \frac{1}{2}\int_{t_0}^{\infty}\left[x^T Q(x)x + u^T R(x)u\right]dt$$

The state dependent weighting matrices Q(x) and R(x) can be chosen to realize the desired performance objectives. In order to ensure local stability, the matrix Q(x) is required

to be positive semidefinite for all x and the matrix R(x) is required to be positive definite for all x.

Next, a state dependent algebraic Riccati equation:

$$A^T(x)P(x) + P(x)A(x) - P(x)B(x)R^{-1}(x)B^T(x)P(x) + Q(x) = 0$$

is formulated and is solved for a positive definite state dependent matrix P(x). The nonlinear state variable feedback control law is then constructed as:

$$u = -R^{-1}(x)B^T(x)P(x)x$$

Cloutier *et al*. (1996) have shown that this control law is locally stable and optimal with respect to the infinite time performance index. Moreover, Cloutier *et al*. (1996) have shown that the SDRE control laws are globally stable if the following condition is satisfied:

$$\dot{P} - Q(x) - P(x)B(x)R^{-1}(x)B^T(x)P(x) < 0$$

This completes the basic SDRE design procedure. Additional sophistication can be introduced in the SDRE design approach by including state estimators, and frequency weighting terms in the performance index. If adequate computational resources are available, the design problem can also be cast as an H• design problem. An excellent overview of the SDRE design technique can be found in Cloutier (1997).

It may be observed that the crucial part of the control law derivation is the solution of the state dependent Riccati equation. In rare situations, this Riccati equation may be solvable in closed-form. In most situations, however, this equation must be numerically solved at each sample. A flow chart illustrating the steps involved in the computation of the SDRE control laws is given in Figure 4.

At each sample, the state vector obtained from feedback sensors or estimators is used to compute the SDC matrices, which are then used to find the state dependent gains. The product of the state dependent gains and the state vector then yields the control variables. Due to the requirement for real-time solution of a Riccati equation, the SDRE approach demands significant amount of computational resources for implementation.

The SDRE methodology will be specifically tailored for use in the development of integrated guidance/control system in the following section.

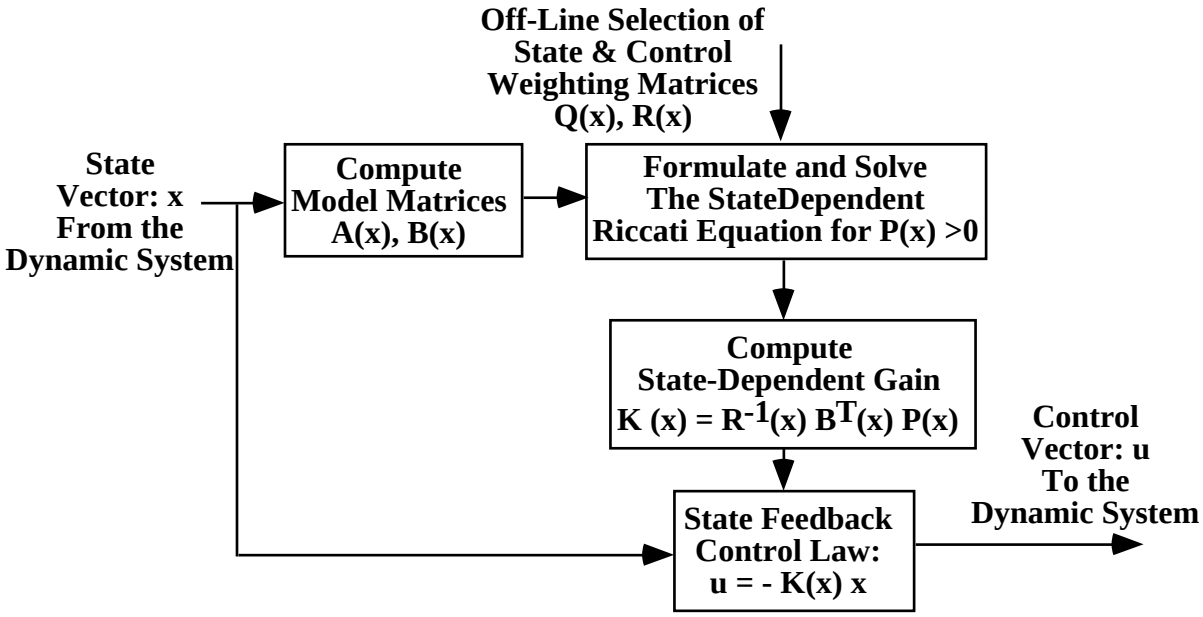

Fig. 4. SDRE Control Law Computations

3.2. Missile Model in State Dependent Coefficient Form

In order to apply the SDRE technique for integrated guidance/control system, the missile equations of motion presented in Section 2 will next be placed in the SDC form. As indicated in the previous section, since the missile is a multivariable system, infinite number of SDC forms can be found for this model. Mracek and Cloutier (1997) presents one of the possible SDC forms for the missile model. The state variables chosen in that work were the body rates, Mach number, angle of attack and the angle of sideslip. Note that Mracek and Cloutier (1997) treated only the autopilot design problem, and did not include the missile translational dynamics in the formulation.

Due to the particular choice of state variables, the SDC parameterization approach presented in Mracek and Cloutier (1997) requires the missile aerodynamic model to be specified in a polynomial form. This may not be acceptable in situations where the design has to be based on non-smooth table look-up aerodynamic data obtained from wind tunnel tests.

An alternate SDC form for the missile equations of motion will be presented in the following. This approach has the advantage of allowing the designer to work with the original set of state variables, while enabling the use of aerodynamic models of arbitrary structure. Thus, the SDC form presented here can be considered to have a more general character. It is important to observe that the SDRE design technique requires the control

variables to appear linearly in the SDC equations and alternate state variable selection does not circumvent this limitation.

The three body velocity components, three body angular rates and two body axis referenced position coordinates are used as the state variables in the present formulation. This choice of state variables is motivated by the observation that the dynamic pressure appears linearly in all the aerodynamic force and moment components. If the winds aloft are neglected, the dynamic pressure is the product of the air density and the sum of the square of the velocity components. Consequently, the missile velocity components can be extracted from the equations of motion to yield the SDC form of the equations of motion. This SDC form has the advantage that it can use aerodynamic models of arbitrary complexity, and is uniformly valid for all angles of attack and angles of sideslip. Thus, the present SDC form can be considered to be particularly suitable for use in high angle of attack missile guidance/control law development.

Following the standard practice in missile guidance law and autopilot design, the gravitational force contributions to the equations of motion will be dropped from consideration. The state vector and the control vector for the SDC model are chosen to be: $x = [P\ \mathrm{Q}\ \mathrm{R}\ \mathrm{U}\ \mathrm{V}\ \mathrm{W}\ \ \mathrm{Y_b}\ \mathrm{Z_b}]^T$, $u = [\delta_{\mathrm{Q}}\ \delta_{\mathrm{R}}\ \delta_{\mathrm{P}}]^T$. Using the missile equations of motion given in Section 2, the elements of the system matrix A(x) can be found to be:

$$A(1,1) = A(1,2) = A(1,3) = 0$$

$$A(1,4) = \frac{1}{I_x}\frac{\rho s l}{2}\left(a_{1_{C_l}}\alpha + a_{2_{C_l}}\beta + a_{3_{C_l}}\alpha^3 + a_{4_{C_l}}\beta^3\right)U$$

$$A(1,5) = \frac{1}{I_x}\frac{\rho s l}{2}\left(a_{1_{C_l}}\alpha + a_{2_{C_l}}\beta + a_{3_{C_l}}\alpha^3 + a_{4_{C_l}}\beta^3\right)V$$

$$A(1,6) = \frac{1}{I_x}\frac{\rho s l}{2}\left(a_{1_{C_l}}\alpha + a_{2_{C_l}}\beta + a_{3_{C_l}}\alpha^3 + a_{4_{C_l}}\beta^3\right)W$$

$$A(1,7) = A(1,8) = 0$$

$$A(2,1) = -\frac{(I_x - I_z)}{I_y}R,\ A(2,2) = A(2,3) = 0$$

$$A(2,4) = \frac{1}{I_y}\frac{\rho s l}{2}\left(a_{1_{C_m}}\alpha + a_{2_{C_m}}\beta + a_{3_{C_m}}\alpha^3 + a_{4_{C_m}}\beta^3\right)U$$

$$A(2,5) = \frac{1}{I_y}\frac{\rho s l}{2}\left(a_{1_{C_m}}\alpha + a_{2_{C_m}}\beta + a_{3_{C_m}}\alpha^3 + a_{4_{C_m}}\beta^3\right)V$$

$$A(2,6)=\frac{1}{I_y}\frac{\rho s l}{2}\left(a_{1_{C_m}}\alpha+a_{2_{C_m}}\beta+a_{3_{C_m}}\alpha^3+a_{4_{C_m}}\beta^3\right)W$$

$$A(2,7)=A(2,8)=0$$

$$A(3,1)=-\frac{(I_y-I_x)}{I_z}Q\,,\ A(3,2)=A(3,3)=0$$

$$A(3,4)=\frac{1}{I_z}\frac{\rho s l}{2}\left(a_{1_{C_n}}\alpha+a_{2_{C_n}}\beta+a_{3_{C_n}}\alpha^3+a_{4_{C_n}}\beta^3\right)U$$

$$A(3,5)=\frac{1}{I_z}\frac{\rho s l}{2}\left(a_{1_{C_n}}\alpha+a_{2_{C_n}}\beta+a_{3_{C_n}}\alpha^3+a_{4_{C_n}}\beta^3\right)V$$

$$A(3,6)=\frac{1}{I_z}\frac{\rho s l}{2}\left(a_{1_{C_n}}\alpha+a_{2_{C_n}}\beta+a_{3_{C_n}}\alpha^3+a_{4_{C_n}}\beta^3\right)W$$

$$A(3,7)=A(3,8)=0$$

$$A(4,1)=0\,,\ A(4,2)=-W\,,\ A(4,3)=V$$

$$A(4,4)=-\frac{\rho s}{2m}\left(a_{0_{C_A}}+a_{1_{C_A}}|\alpha|+a_{2_{C_A}}|\beta|+a_{3_{C_A}}|\alpha\beta|\right)U$$

$$A(4,5)=-\frac{\rho s}{2m}\left(a_{0_{C_A}}+a_{1_{C_A}}|\alpha|+a_{2_{C_A}}|\beta|+a_{3_{C_A}}|\alpha\beta|\right)V$$

$$A(4,6)=-\frac{\rho s}{2m}\left(a_{0_{C_A}}+a_{1_{C_A}}|\alpha|+a_{2_{C_A}}|\beta|+a_{3_{C_A}}|\alpha\beta|\right)W$$

$$A(4,7)=A(4,8)=0$$

$$A(5,1)=W\,,\ A(5,2)=0\,,\ A(5,3)=-U$$

$$A(5,4)=\frac{\rho s}{2m}\left(a_{1_{C_Y}}\alpha+a_{2_{C_Y}}\beta+a_{3_{C_Y}}\alpha^3+a_{4_{C_Y}}\beta^3\right)U$$

$$A(5,5)=\frac{\rho s}{2m}\left(a_{1_{C_Y}}\alpha+a_{2_{C_Y}}\beta+a_{3_{C_Y}}\alpha^3+a_{4_{C_Y}}\beta^3\right)V$$

$$A(5,6)=\frac{\rho s}{2m}\left(a_{1_{C_Y}}\alpha+a_{2_{C_Y}}\beta+a_{3_{C_Y}}\alpha^3+a_{4_{C_Y}}\beta^3\right)W$$

$$A(5,7)=A(5,8)=0$$

$$A(6,1)=-V\,,\ A(6,2)=U\,,\ A(6,3)=0$$

$$A(6,4)=-\frac{\rho s}{2m}\left(a_{1_{C_N}}\alpha+a_{2_{C_N}}\beta+a_{3_{C_N}}\alpha^3+a_{4_{C_N}}\beta^3\right)U$$

$$A(6,5)=-\frac{\rho s}{2m}\left(a_{1_{C_N}}\alpha+a_{2_{C_N}}\beta+a_{3_{C_N}}\alpha^3+a_{4_{C_N}}\beta^3\right)V$$

$$A(6,6) = -\frac{\rho s}{2m}\left(a_{1_{C_N}}\alpha + a_{2_{C_N}}\beta + a_{3_{C_N}}\alpha^3 + a_{4_{C_N}}\beta^3\right)W$$

$$A(6,7) = A(6,8) = 0$$

$$A(7,1) = -Z_b,\ A(7,2) = 0,\ A(7,3) = -X_b$$

$$A(7,4) = 0,\ A(7,5) = 1,\ \mathrm{A}(7,6) = \mathrm{A}(7,7) = \mathrm{A}(7,8) = 0$$

$$\mathrm{A}(8,1) = -\mathrm{Y_b},\ A(8,2) = X_b,\ A(8,3) = 0$$

$$A(8,4) = A(8,5) = 0,\ A(8,6) = 1,\ A(8,7) = A(8,8) = 0$$

The elements of the control influence matrix B(x) in the SDC model are:

$$B(1,1) = \frac{1}{I_x}\bar{q}sl\ a_{5_{C_l}},\ B(1,2) = \frac{1}{I_x}\bar{q}sl\ a_{6_{C_l}},\ B(1,3) = \frac{1}{I_x}\bar{q}sl\ a_{7_{C_l}}$$

$$B(2,1) = \frac{1}{I_y}\bar{q}sl\ a_{5_{C_m}},\ B(2,2) = \frac{1}{I_y}\bar{q}sl\ a_{6_{C_m}},\ B(2,3) = \frac{1}{I_y}\bar{q}sl\ a_{7_{C_m}}$$

$$B(3,1) = \frac{1}{I_z}\bar{q}sl\ a_{5_{C_n}},\ B(3,2) = \frac{1}{I_z}\bar{q}sl\ a_{6_{C_n}},\ B(3,3) = \frac{1}{I_z}\bar{q}sl\ a_{7_{C_n}}$$

$$B(5,1) = \frac{\bar{q}s}{m}a_{5_{C_Y}},\ B(5,2) = \frac{\bar{q}s}{m}a_{6_{C_Y}},\ B(5,3) = \frac{\bar{q}s}{m}a_{7_{C_Y}}$$

$$B(6,1) = -\frac{\bar{q}s}{m}a_{5_{C_N}},\ B(6,2) = -\frac{\bar{q}s}{m}a_{6_{C_N}},\ B(6,3) = -\frac{\bar{q}s}{m}a_{7_{C_N}}$$

$$B(7,1) = B(7,2) = B(7,3) = 0$$

$$B(8,1) = B(8,2) = B(8,3) = 0$$

Numerical evaluations at several values of the state variables have shown that the missile model in the above SDC form is completely controllable. This missile model will be used next for the development of the integrated guidance/control system.

3.3. LQR - SDRE Design of Integrated Guidance/Control System

After transforming the missile model into the SDC form, the next major responsibility of the designer is to select the state weighting matrix Q(x) and the control weighting matrix R(x). As indicated elsewhere in this chapter, Q(x) is required to be positive semidefinite for all expected values of x, and R(x) is required to be positive definite for all expected values of x. Selecting matrix functions that meet these requirements for all values of the state vector is not generally practical. The approach advocated in Mracek and Cloutier (1997) and

that employed here is to select Q and R to be constant matrices at first, and then explore the payoffs in scheduling these constant matrices as functions of key state vector components.

Two major criteria have been found useful in the selection of Q(x), R(x) weighting matrices. Unlike the classical linear-quadratic regulator problem, assuring the positive semidefiniteness of the Q matrix and the positive definiteness of the R matrix are not sufficient to guarantee global stability. In the presence of large variations in the state variables, stability can be guaranteed only if the Riccati matrix P(x) satisfies the inequality (Cloutier, 1997):

$$\dot{P} - Q(x) - P(x)B(x)R^{-1}(x)B^{T}(x)P(x) < 0$$

This criterion can be used to iteratively refine the selection of the Q(x), R(x) matrices. Initial Q and R can be selected to be identity matrices. Test runs can then be used to determine the rate of change of the P(x) matrix, and then to make modifications to the Q, R matrices. This iterative refinement will allow the selection of Q and R matrices that ensure the closed-loop system stability for all expected values of x. However, this choice of Q(x) and R(x) may not produce the desired performance characteristics for the integrated guidance/control law.

A second guideline for the selection of the Q(x) and R(x) matrices is based on Bryson's rule (Bryson and Ho, 1975) for the design of linear quadratic regulators. According to Bryson and Ho (1975), the Q and R matrices in the infinite-time linear-quadratic optimal control problem can be chosen as:

$$Q(x) = diag\left[\frac{1}{P_{\max}^2 t_s} \; \frac{1}{Q_{\max}^2 t_s} \; \frac{1}{R_{\max}^2 t_s} \; \frac{1}{U_{\max}^2 t_s} \; \frac{1}{V_{\max}^2 t_s} \; \frac{1}{W_{\max}^2 t_s} \; \frac{1}{Y_{b\max}^2 t_s} \; \frac{1}{Z_{b\max}^2 t_s}\right]$$

$$R(x) = diag\left[\frac{1}{\delta_{Q\max}^2 t_s} \; \frac{1}{\delta_{R\max}^2 t_s} \; \frac{1}{\delta_{P\max}^2 t_s}\right]$$

The subscript "max" denotes the maximum permissible values, and t_s is the desired settling time. For the present research, the choice of the weighting matrices that resulted in reasonably good performance characteristics turned out to be:

$$Q = diagonal\left(\left[100, 100, 100, \; 0, 1.0e-08, 1.0e-08, 2.0e+01, 2.0e+01\right]\right)$$

R = 1e5*diagonal([1 1 1]);

These matrices were obtained after several numerical experiments. Note that the state weight corresponding to the velocity component U has been set to zero, due to the fact that the integrated guidance/control system is not expected to control this state variable. Although it is desirable to change the weighting matrices as a function of the engagement

geometry, due to the preliminary nature of the present research, the weighting matrices are maintained constant throughout an engagement.

In future work, one of the criteria for the selection of state dependent weighting matrices could be the range to the target. For instance, lower state weights can be used when the missile is far away from the target, and as the missile approaches the target, the state weights can be tightened. A reverse strategy can be used for the control weighting matrix: higher magnitudes when the missile is far from the target, and smaller magnitudes as the missile approaches the target. This will ensure agile behavior while avoiding unnecessary actuator saturation. In this way, the closed-loop system response can be tailored to approximate the behavior of a finite time-horizon integrated guidance/control law. Note that such range or time-to-go based scheduling strategy is automatically built into more traditional guidance laws like the proportional navigation and augmented proportional navigation guidance laws (Bryson and Ho, 1975).

A more flexible design approach to ensure agile missile response is to employ a command generation system in the integrated guidance/control loop. The command generator will allow a control system to use high loop gains while providing a saturation-free closed-loop system response. In the integrated guidance/control problem, the command generator will enable the implementation of desired terminal conditions. The following section will discuss the command generator in further detail.

3.4. Command Generation

Since the SDRE formulation is essentially an infinite time formulation, when faced with an error, it will immediately attempt to correct the error. This can lead to actuator saturation followed by large transients in the state variables, with the potential for the closed-loop system to go unstable. On the other hand, slowing the system down to prevent actuator saturation can lead to sluggish system response, with the possibility for large miss distances. The use of a command generator can alleviate these difficulties.

The design flexibility available with the use of a command generator has been amply demonstrated in linear system design literature (Wolovich, 1994). The two degree-of-freedom design philosophy[12] employs a command shaping network to obtain the desired tracking characteristics, and a feedback compensator is used to achieve the desired closed-loop system stability and robustness characteristics. These two subsystems can be used to achieve overall design objectives without sacrificing stability, robustness or the tracking

behavior. From an implementation point of view, the two degree-of-freedom design process allows high gain control laws that will not saturate the actuators.

In the integrated guidance/control problem, the command generator uses the current target position and velocity components with respect to the missile, desired boundary conditions and expected point of interception to synthesize a geometric command profile. The command profile can be re-computed at each time instant, allowing for the correction of computational errors made during the previous step. Such an approach will distribute the control power requirements over the interception time, thereby allowing a fast responding closed-loop system that does not produce unnecessary actuator saturation.

The command profile can be computed from the initial conditions and the interception requirements. The initial conditions on the missile position and velocity are specified, and the terminal position of the missile must coincide with the target. In the case of a terminal aspect angle requirement, the terminal velocity component may also be specified. Since there are four conditions to be satisfied, a cubic polynomial is necessary to represent the command profile. Note that if the terminal aspect angle requirement is absent, a quadratic polynomial is sufficient for generating commands. The independent variable of the cubic polynomial can be chosen as the state variable not being controlled, namely, the position difference between the missile and the target along the X body axis of the missile. Additionally, since the desired final miss distance is zero, the leading term in the cubic polynomial can be dropped. With this, the commanded trajectory profiles will be of the form:

$$Y_{bc} = a_1 X_b + a_2 X_b^2 + a_3 X_b^3$$

$$Z_{bc} = b_1 X_b + b_2 X_b^2 + b_3 X_b^3$$

Figure 5 illustrates a typical commanded trajectory profile.

The coefficients a_1, a_2, a_3, b_1, b_2, b_3 can be computed using the boundary conditions as:

$$a_1 = \frac{\dot{Y}_{bf}}{\dot{X}_{bf}}, \quad b_1 = \frac{\dot{Z}_{bf}}{\dot{X}_{bf}}$$

$$a_2 = \frac{3}{X_b^2}\left[Y_{b0} - \frac{\dot{Y}_{bf}}{\dot{X}_{bf}} X_{b0}\right] - \frac{1}{X_{b0}\dot{X}_{b0}}\left[\dot{Y}_{b0} - \frac{\dot{Y}_{bf}}{\dot{X}_{bf}}\dot{X}_{b0}\right]$$

$$b_2 = \frac{3}{X_b^2}\left[Z_{b0} - \frac{\dot{Z}_{bf}}{\dot{X}_{bf}} X_{b0}\right] - \frac{1}{X_{b0}\dot{X}_{b0}}\left[\dot{Z}_{b0} - \frac{\dot{Z}_{bf}}{\dot{X}_{bf}}\dot{X}_{b0}\right]$$

$$a_3 = -\frac{2}{X_{b0}^3}\left[Y_{b0} - \frac{\dot{Y}_{bf}}{\dot{X}_{bf}} x_{b0}\right] + \frac{1}{X_{b0}^2 \dot{X}_{b0}}\left[\dot{Y}_{b0} - \frac{\dot{Y}_{bf}}{\dot{X}_{bf}} \dot{X}_{b0}\right]$$

$$b_3 = -\frac{2}{X_{b0}^3}\left[Z_{b0} - \frac{\dot{Z}_{bf}}{\dot{X}_{bf}} X_{b0}\right] + \frac{1}{X_{b0}^2 \dot{X}_{b0}}\left[\dot{Z}_{b0} - \frac{\dot{Z}_{bf}}{\dot{X}_{bf}} \dot{X}_{b0}\right]$$

Note that the command profiles do not require the specification of time-to-go, but need the specification of the closing rate along the X-body axis. Target interception will be achieved if the SDRE integrated control law closely tracks the commands. In case of agile targets, it may be useful to include a certain amount of anticipatory characteristics in the command generator. This will effectively introduce additional "phase lead" in the integrated guidance/control loop, potentially resulting in decreased miss distances. These and other advanced command generation concepts will be investigated during future research.

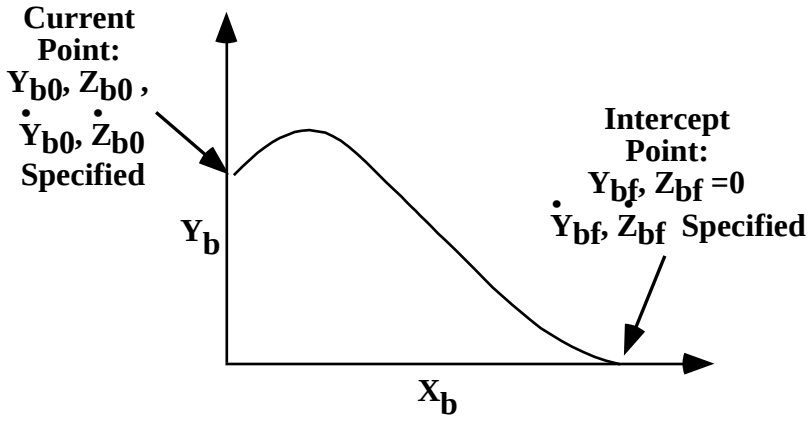

Fig. 5. Commanded Trajectory Profile

Although the cubic polynomial command generators were implemented in the pitch and yaw planes, in the interests of maintaining simplicity during the present research, only the leading terms were used for generating the commands. The next section will present the simulation results using the integrated guidance/control law for three engagement scenarios.

3.5. Integrated Guidance/Control System Performance Evaluation

As discussed in the previous sections, the integrated SDRE guidance/control system consists of a command generator, and an SDRE control law. A schematic block diagram of the integrated guidance/control system is given in Figure 6.

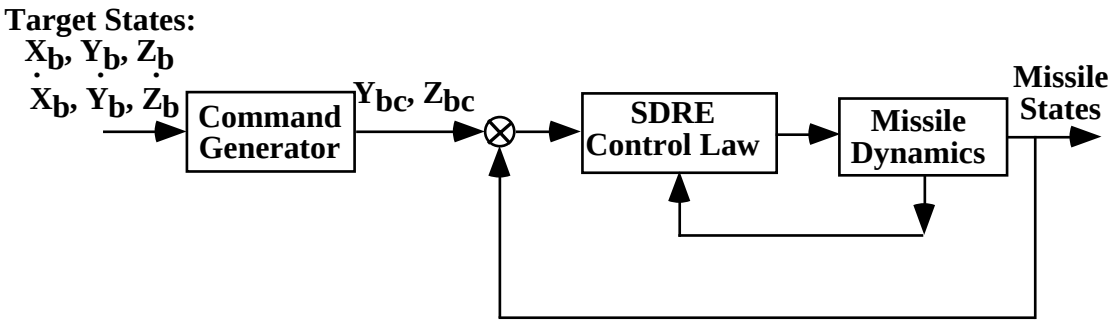

Fig. 6. Integrated Guidance/Control System

A six degree-of-freedom missile simulation set up during earlier research projects (Menon *et al.*, 1996)is used to evaluate the performance of the integrated guidance/control law. This simulation incorporates a nonlinear missile model, together with sensor/actuator dynamics and vehicle flexibility effects. In the interests of saving computational time, the sensor/actuator dynamics and the flexibility effects are not included in the present simulation runs. A point-mass target model is included in the simulation runs. Euler integration method with a step size of 1 millisecond is used in all the simulation runs.

The engagement scenarios illustrated here assume that the missile is flying at an altitude of 50000 feet, and at a Mach number of 5. The airframe is initially trimmed at an angle of attack and angle of sideslip of 0.1 degrees. The missile down range and cross-range positions in the inertial frame at the initial time instant are assumed to be zero. The results for three engagement scenarios will be given in the following.

3.5.1. Crossing Target

The first scenario chosen to illustrate the performance of the integrated SDRE guidance/control law is that of a crossing target. The target is assumed to be located at 10000 feet down range, -300 feet cross range and 50300 feet in altitude. It has 100 feet/s velocity along the cross range and altitude directions. The missile/target trajectories in the vertical and horizontal plane are given in Figure 7. The target trajectories are denoted by dashed lines in these figures.

The oscillations observed in the lateral components at the initial time are the result of lightly damped body rate dynamics. This low damping in the body rate dynamics is largely the result of trying to obtain fast response using pure proportional feedback. These responses can be further refined by a more careful choice of the weighting matrices in the SDRE design process, and through the use of dynamic compensators. Frequency weighting terms in the performance index can also help realize the desired closed-loop system response.

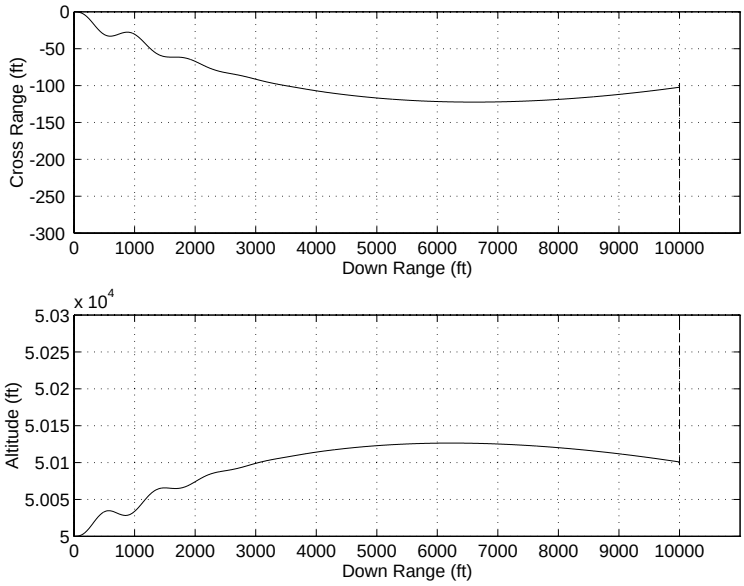

Fig. 7. Interception of a Crossing Target

The interception occurred at about 2.1 seconds, with a miss distance of about 20 feet. Analysis has shown that the miss distance arises primarily due to the differences in the performance of the integrated guidance/control system between the vertical and horizontal planes, and not because of any inherent limitations of the SDRE control law formulation. Thus, the integrated control system drove the Y_b error to zero a few milliseconds before driving the Z_b error to zero. Note that this miss distance can be made arbitrarily small through the use of an improved command generator, perhaps including a certain amount of "lead". Additional refinements include the use of integral feedbacks on the two position components. These improvements will be pursued during future research.

The missile body velocity components corresponding to this intercept scenario are given in Figure 8.

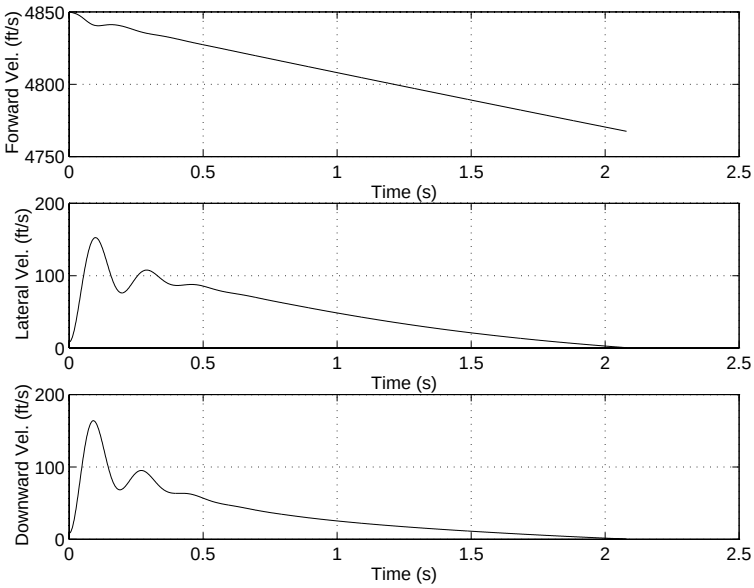

Fig. 8. Temporal Evolution of Body Velocity Components

Note that the missile velocity along the longitudinal axis falls continuously due to the axial force. The changes in the longitudinal velocity induced by the lateral maneuvers can be clearly identified at the beginning of the longitudinal velocity history. The lateral velocity components show larger changes at the beginning and gradually approach zero near the intercept. Note that this behavior will change if the weighting matrices are made functions of time-to-go or range-to-go.

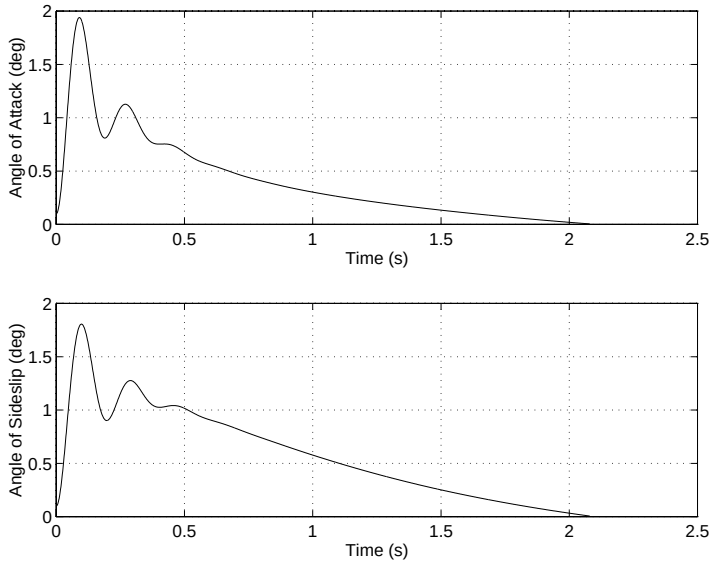

Fig. 9. Angle of Attack and Angle of Sideslip Histories

The angle of attack and angle of sideslip histories given in Figure 9 mirror the lateral velocity component variations.

The missile roll, pitch, yaw rate histories are presented in Figure 10. Corresponding fin deflections are given in Figure 11.

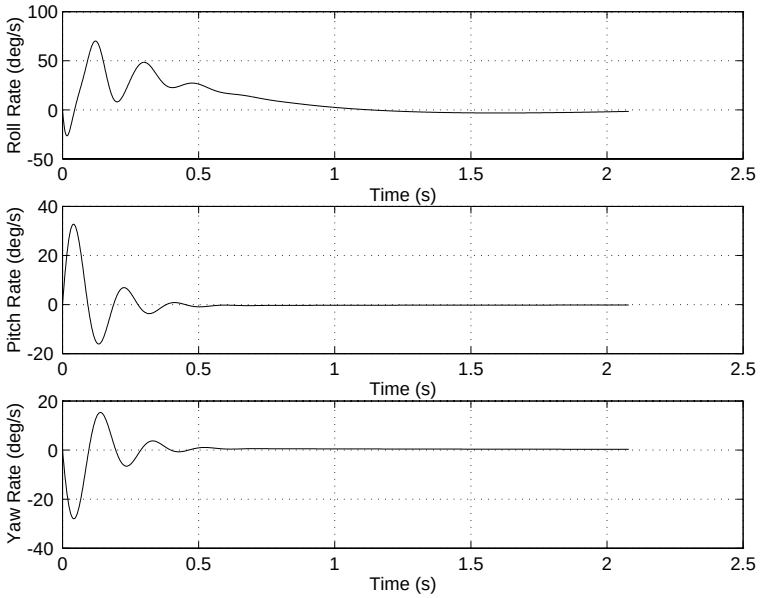

Fig. 10. Roll, Pitch, Yaw Rate Histories

It may be observed that the body rates show a large initial transient, followed by rather modest variations throughout the interception. The activity observed in the roll rate arises primarily due to the coupling of this axis with the pitch and yaw axes through angle of attack, angle of sideslip and the fin deflections.

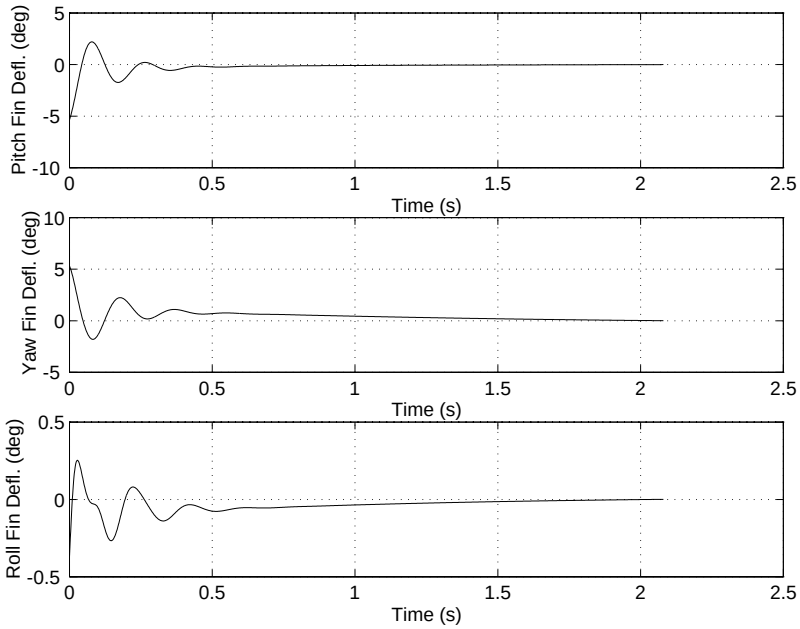

Fig. 11. Fin Deflection Histories

3.5.2. Weaving Target

A weaving target model discussed in Section 2 is used to evaluate the response of the SDRE integrated guidance/control system. The missile initial conditions were identical to the two previous cases. The target is assumed to be located at 10000 feet in down range, 300 feet in cross range, and 50300 feet altitude. It is assumed to have a down range velocity of 3000 feet/s, cross range velocity of 40 feet/s and a descent rate of 40 feet/s. A weaving amplitude of 50 feet, with a frequency of 2 rad/s is introduced in the horizontal plane. The weaving frequency amplitude and frequency are chosen based on Reference 3.

The missile-target trajectories in the horizontal and the vertical planes are presented in Figure 12. The interception required about 5.8 seconds, and the terminal miss distance was about 9 feet.

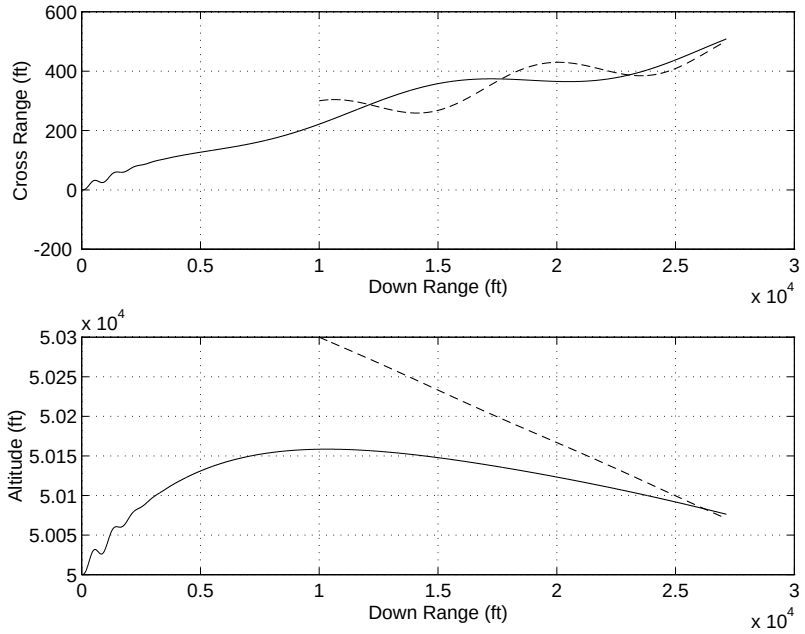

Fig. 12. Interception of a Weaving Target

As in the two previous cases, the miss distance could be largely attributed to the differences in performance between the vertical and horizontal channels. Improved state-control weight selection and controller scheduling with respect to range or time-to-go will result in significant improvements in the miss distance. A command generator including some lead can also contribute towards reducing the miss distance.

The components of the body velocity vector are given in Figure 13. Unlike the two previous scenarios, the lateral velocity components are continuously changing. The angle of attack and angle of sideslip histories corresponding to this engagement are illustrated in

Figure 14. Roll, pitch, yaw body rates are illustrated in Figure 15. Corresponding fin deflections are given in Figure 16.

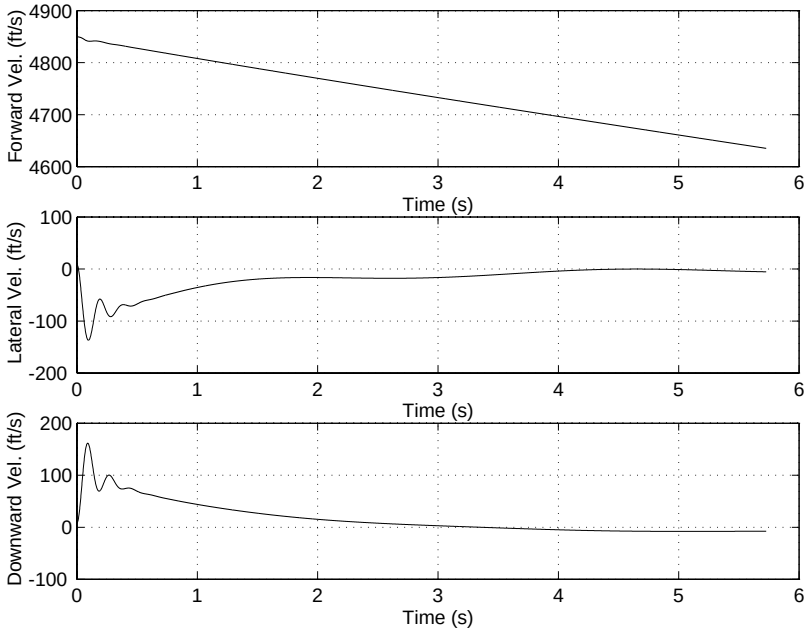

Fig. 13. Temporal Evolution of Body Velocity Components

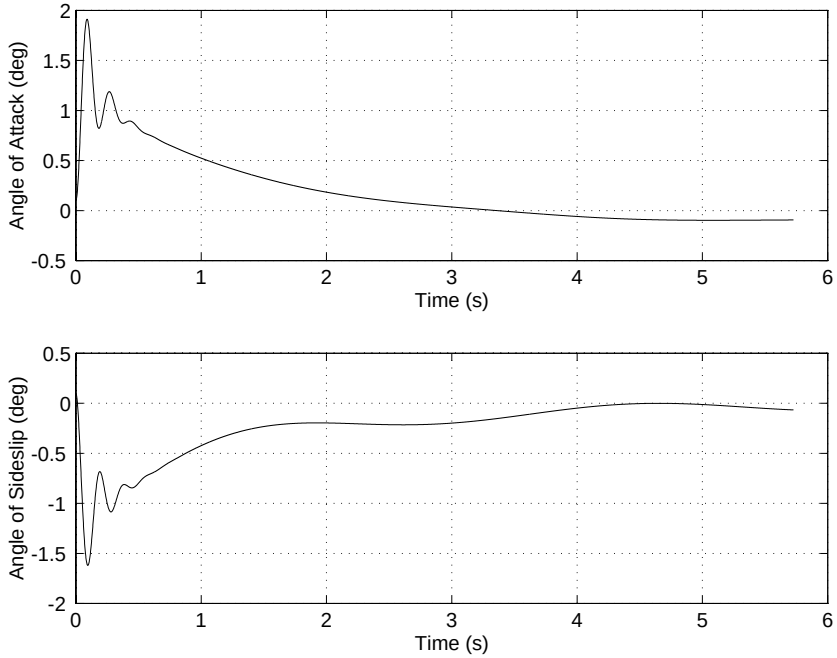

Fig. 14. Angle of Attack and Angle of Sideslip Histories

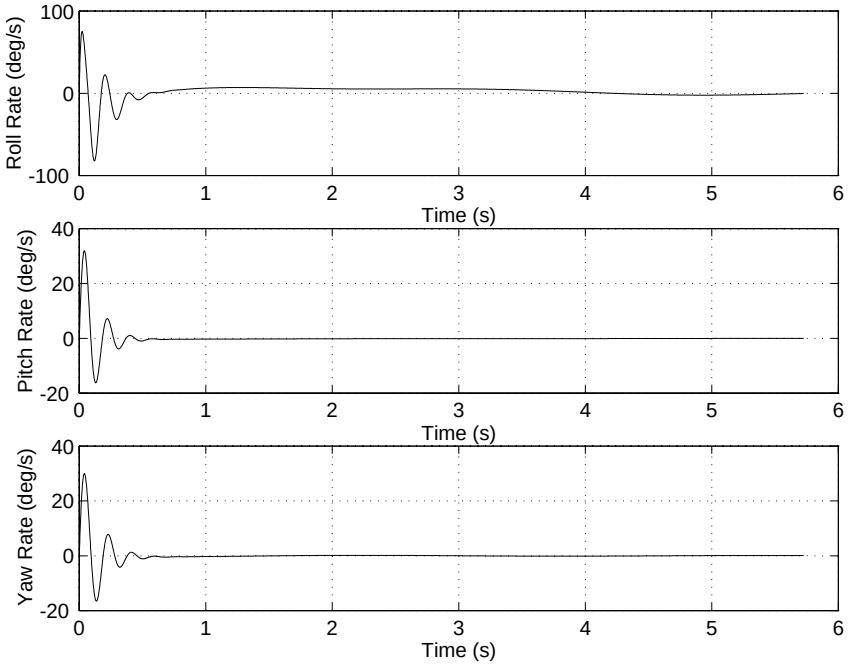

Fig. 15. Roll, Pitch, Yaw Rate Histories

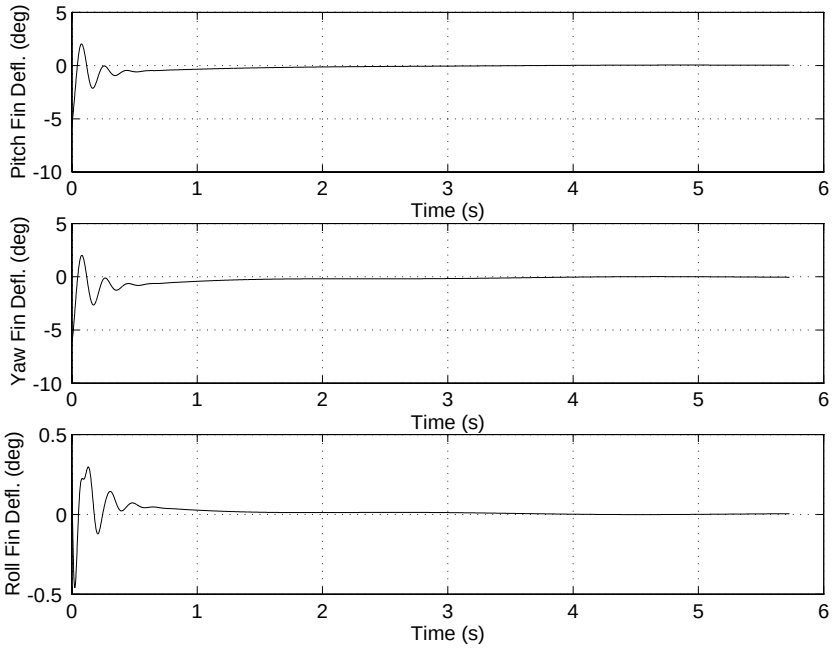

Fig. 16. Fin Deflection Histories

As with the previous engagement scenario, due to the reactive nature of the SDRE guidance/control law, most of the control activity is at the beginning of the engagement. Scheduling the weighting matrices with respect to time-to-go or range to the target will change this behavior.

5. Conclusions

State Dependent Riccati Equation (SDRE) method for designing integrated guidance/control systems for ship defense missiles was discussed this paper. A new state dependent coefficient form of the missile model was derived, and the integrated missile guidance/control system design was formulated as an infinite time-horizon optimal control problem. The need for a command generator was motivated, and a cubic command generator development was presented. Introduction of the command generator allowed the control loop to use high gain without resulting in actuator saturation. The command generator was also shown to be useful for meeting terminal aspect angle constraints. The SDRE integrated guidance/control law performance was demonstrated in a nonlinear six degree-of-freedom missile simulation for a crossing target and a weaving target. Methods for further refining the SDRE integrated guidance/control law were discussed.

The analysis and numerical results presented in this paper amply demonstrate the feasibility of designing integrated guidance/control systems for the next generation high-performance missile systems. Integrated design methods have the potential for enhancing missile performance while simplifying the design process. This can result in a lighter, more accurate missile system for effective defense against various Naval threats expected in the future.

7. References

Ohlmeyer, E. J. (1996). "Root-Mean-Square Miss Distance of Proportional Navigation Missile Against Sinusoidal Target", *Journal of Guidance, Control, and Dynamics*, Vol. 19, May-June, pp. 563-568.

Bibel, J. E., Malyevac, D. S., and Ohlmeyer, E. J. (1994). "Robust Flight Control for Surface Launched Tactical Missiles", *Naval Surface Warfare Center Dahlgren Division Technical Digest*, September.

Chadwick, W. R. (1994). "Reentry Flight Dynamics of a Non-Separating Tactical Ballistic Missile", *Proceedings of AIAA/BMDO Interceptor Technology Conference*, San Diego, CA.

Zarchan, P. (1995). "Proportional Navigation and Weaving Targets", *Journal of Guidance, Control, and Dynamics*, Vol. 18, No. 5, pp. 969-974.

Garg, S. (1993). "Robust Integrated Flight/Propulsion Control Design for a STOVL Aircraft using H-Infinity Control Design Techniques", *Automatica*, Vol. 29, No. 1, pp. 129-145.

Menon, P. K., and Iragavarapu, V. R. (1995) “Computer-Aided Design Tools for Integrated Flight/Propulsion Control System Synthesis”, Final Report Prepared under NASA Lewis Research Center Contract No. NAS3-27578, June.

Menon, P. K., and Iragavarapu, V. R. (1998). *“Adaptive Techniques for Multiple Actuator Blending”, AIAA* Guidance, Navigation, and Control Conference, August 10-12, Boston, MA.

Cloutier, J. R., D’Souza, C. N., and Mracek, C. P. (1996). “Nonlinear Regulation and Nonlinear H• Control Via the State-Dependent Riccati Equation Technique”, *Proceedings of the International Conference on Nonlinear Problems in Aviation and Aerospace*, Daytona Beach, FL, May.

Mracek, C.P. and Cloutier, J.R. (1997). “Missile Longitudinal Autopilot Design using the State Dependent Riccati Equation Method”, *Proceedings of the 1997 American Control Conference*, June 4 - 6, Albuquerque, NM.

Cloutier, J.R. (1997). “State-Dependent Riccati Equation Techniques: An Overview”, *Proceedings of the 1997 American Control Conference*, June 4 - 6, Albuquerque, NM.

Menon, P. K., and Iragavarapu, V. R. (1996). “Robust Nonlinear Control Technology for High-Agility Missile Interceptors”, *Optimal Synthesis* Report No. 005, Prepared Under NSWCDD Phase I SBIR Contract, July.

Wolovich, W. A. (1994). *Automatic Control Systems*, Harcourt-Brace, New York, NY.

Bryson, A. E., and Ho, Y. C. (1975). *Applied Optimal Control*, Hemisphere, New York.